

Supporting Information

Acoustic droplet vaporization of perfluorohexane emulsions is induced by heterogeneous nucleation at an ultrasonic frequency of 1.1 MHz

R. Ramesh,^{†,‡,Ⓜ} C. Thimonier,^{†,¶,‡,Ⓜ} S. Desgranges,[§] V. Faugeras,[‡] F. Coulouvrat,^{||} J. Laurent,[⊥] G. Marrelec,[†] C. Contino-Pépin,[§] W. Urbach,[‡] C. Tribet,[#] and N. Taulier^{*,†}

[†]*Sorbonne Université, CNRS, INSERM, Laboratoire d'Imagerie Biomédicale, LIB, F-75006 Paris, France.*

[‡]*Laboratoire de Physique de l'École Normale Supérieure, ENS, Université PSL, CNRS, Sorbonne Université, Université de Paris Cité, F-75005 Paris, France.*

[¶]*Département de Chimie, P.A.S.T.E.U.R., École Normale Supérieure, Université PSL, Sorbonne Université, CNRS, Paris 75005, Paris, France.*

[§]*Avignon Université, Équipe Systèmes Amphiphiles bioactifs et Formulations Eco-compatibles, UPRI, 84000 Avignon, France.*

^{||}*Sorbonne Université, Institut Jean le Rond d'Alembert, CNRS, 4 place Jussieu, 75005 Paris France.*

[⊥]*PMMH, ESPCI, Université PSL, CNRS, Sorbonne Université, Université de Paris Cité, 75005 Paris France.*

[#]*PASTEUR, Département de chimie, École normale supérieure, PSL University, Sorbonne Université, CNRS, 75005 Paris, France*

[Ⓜ]*Authors contributed equally*

E-mail: nicolas.taulier@cnrs.fr

Annex

Probability of vaporization

We assume that each droplet can vaporize independently of what happens with the other ones. Indeed, low droplet volume fractions were used to minimize interactions between droplets as well as between vaporization events. Under this assumption of independence, the probability to observe k vaporization events from the n droplets is given by the binomial distribution with parameters n and $p^{(1)}$. From this model, the probability to obtain no vaporization event is given by $[1 - p^{(1)}]^n$, and the probability to observe at least one vaporization event by

$$p_{\geq 1}^{(n)} = 1 - [1 - p^{(1)}]^n. \quad (\text{S1})$$

Note that for $p^{(1)}$ small and n large such that $np^{(1)}$ remains moderate, a good approximation of the binomial distribution is the Poisson distribution. In Eq. S1, $p^{(1)}$ is an increasing function of pressure P with values in $[0,1]$, which we can express as $p^{(1)} = \Psi(P)$. If $\Psi(P)$ is considered as the cumulative distribution function (cdf) of a random variable X , then Eq. S1 shows that $p_{\geq 1}^{(n)}$ is the expression for the cdf corresponding to the minimum of n independent and identically distributed (i.i.d.) samples of X (Eq. 9.1.1 in¹). Extreme value theory then shows that, when n becomes large, $p_{\geq 1}^{(n)}$ can only converge toward one of three types of distributions depending on $\Psi(P)$ (Section 10.5 in²). In particular, when $\Psi(P)$ belongs to specific families (including the normal, lognormal, maximal Gumbel, minimal Gumbel, maximal Weibull, and maximal Fréchet distributions), the limiting distribution for $p_{\geq 1}^{(n)}$ is the minimal Gumbel distribution with location parameter $\mu^{(n)}$ and scale parameter $\beta^{(n)}$ (Table 9.5 in¹), i.e.,

$$p_{\geq 1}^{(n)} \approx 1 - \exp \left[-e \left(\frac{P - \mu^{(n)}}{\beta^{(n)}} \right) \right], \quad (\text{S2})$$

Furthermore, given $\Psi(P)$, it is possible to provide an asymptotic expression for the parameters of the minimal Gumbel distribution as a function of n . For instance, if $\Psi(P)$ is given

by the error function or, equivalently, an integral Gaussian distribution, with median $P_{0.5}^{(1)}$ and standard deviation $\sigma^{(1)}$, then it can be shown that the parameters $\mu^{(n)}$ and $\beta^{(n)}$ can be expressed as

$$\mu^{(n)} = P_{0.5}^{(1)} - \sigma^{(1)} d_n \quad (\text{S3})$$

and

$$\beta^{(n)} = \sigma^{(1)} c_n, \quad (\text{S4})$$

with

$$c_n = \frac{1}{\sqrt{2 \ln(n)}} \quad (\text{S5})$$

and

$$d_n = \sqrt{2 \ln(n)} - \frac{\ln(\ln(n)) + \ln(4\pi)}{2\sqrt{2 \ln(n)}}. \quad (\text{S6})$$

This result was obtained by combining the asymptotic result regarding the maximum in the case of a standard normal distribution (Example 3.3.29 in³), the relation between maximum and minimum (Section 3.1 in³) as well as the expression of a general normal distribution in terms of a standard normal distribution. Finally, the ADV corresponding to n droplets, which we denote by $P_{0.5}^{(n)}$ here to emphasize the dependence on n , is the median of the Gumbel distribution of Eq. S2, given by

$$P_{0.5}^{(n)} = \mu^{(n)} + \beta^{(n)} \ln(\ln(2)) \quad (\text{S7})$$

$$= P_{0.5}^{(1)} - \sigma^{(1)} [d_n - c_n \ln(\ln(2))], \quad (\text{S8})$$

Probability of nucleation

The stochastic nature of bubble nucleation on exposure to an acoustic wave leads us treat the formation of a nucleus in a given volume as a series of random events. The Poisson distribution law gives the probability q_m of forming exactly m nuclei within a time interval

$\tau^{4,5}$, assuming they occur independently from one another:

$$q_m = \frac{N^m(\tau)e^{-N(\tau)}}{m!}. \quad (\text{S9})$$

Here $N(\tau)$ is the expected average number of nuclei created during the time interval τ . For instance, the probability to form exactly no nucleus is $q_0 = e^{-N(\tau)}$. The sum of all probabilities should be equal to 1:

$$1 = \sum_{i=0}^{\infty} q_i \quad (\text{S10})$$

Thus, the probability to create at least one nucleus is

$$q_{\geq 1} = 1 - q_0 = 1 - e^{-N(\tau)}, \quad (\text{S11})$$

which can be rewrite as

$$N(\tau) = \ln \left(\frac{1}{1 - q_{\geq 1}} \right). \quad (\text{S12})$$

For homogeneous nucleation, the average number of nuclei occurring during a time τ and inside a volume V is related to the volume nucleation rate J through

$$N(\tau) = JV\tau, \quad (\text{S13})$$

while for heterogeneous nucleation, the average number of nuclei during a time τ and on a surface area A is related to the surface nucleation rate Π :

$$N(\tau) = \Pi A\tau. \quad (\text{S14})$$

The nucleation rates depends on the Boltzmann constant k_B , the absolute temperature T , and the energy barrier to be overcome W as follows. In the homogeneous case,

$$J = J_0 \exp \left(-\frac{W^{\text{hom}}}{k_B T} \right), \quad (\text{S15})$$

where⁶

$$J_0 = N_A \rho \sqrt{\frac{2\gamma}{\pi M}}. \quad (\text{S16})$$

N_A is the Avogadro number, ρ the density and M the mass of a molecule (of PFH in our case). In the heterogeneous case,

$$\Pi = \Pi_0 \exp\left(-\frac{W^{\text{het}}}{k_B T}\right), \quad (\text{S17})$$

where⁶

$$\Pi_0 = N^{2/3} \frac{1 - \cos \theta}{2} \sqrt{\frac{2\gamma_{gl}}{\pi M}}. \quad (\text{S18})$$

The rate is null when $\cos \theta = 1$, i.e. when $\theta = 0$ (there is no nucleus) or π (the nucleus is not attached to the surface). Because of the exponential in nucleation rate, changes by several orders of magnitude in the values of J_0 and Π_0 only marginally affect the final results in nucleation rate.

We can thus relate the probability to create at least one nucleus to the rate of nucleation regardless the type of nucleation (homogeneous or heterogeneous) using Eq. S11 and Eq. S15 or S17, and leading to

$$q_{\geq 1} = 1 - e^{-\Omega\tau}, \quad (\text{S19})$$

where Ω is equal to either JV or ΠA depending on whether the nucleation is homogeneous or heterogeneous. The energy required to create at least one nucleus is thus

$$W(q_{\geq 1}) = k_B T \ln \left(\frac{\Omega\tau}{\ln \left(\frac{1}{1-q_{\geq 1}} \right)} \right). \quad (\text{S20})$$

Model of a heterogeneous nucleation on a soft surface

Since the surface is flexible, we hypothesize that the appearance of a nucleus on the surface of a droplet of radius R will lead to the surface deformation. In such a case, the nucleus volume is made of two hemispheres, one of radius r_1 (similar to the radius r defined in

heterogeneous nucleation on solid surface), and a second radius r_2 that is much lower than the droplet radius R (while it is considered to be equal to R when considering a solid surface). The work needed to create a nucleus is

$$W = \gamma_{gl}(r_1)a(\psi, r_1) + \gamma_{gc}(r_2)a(\varphi, r_2) - \gamma_{lc}a(\chi, R) - (P_g - P_l)v + n_{\text{PFH}}(\mu_g - \mu_l) \quad (\text{S21})$$

where the subscripts l , g , and c refers to the liquid PFC, the gaseous PFC, and the glycerol, respectively, v is the volume of the nucleus, $\gamma_{gl}(r_1)$, γ_{lc} and $\gamma_{gc}(r_2)$ are the interfacial free energy per unit area between the liquid and gaseous PFH phase, between the liquid PFH and glycerol, and between the gaseous PFH and glycerol, respectively. These phases are separated from each other by a surface, whose surface area are respectively $a(\psi, r_1)$, $a(\varphi, r_2)$ and $a(\chi, R)$. The total surface area of the nucleus is $a = a(\psi, r_1) + a(\varphi, r_2)$. For perfluorohexane, the value of vapor pressure is equal to $P_v \approx 29.33$ kPa.

The volume of a nuclei is (we used the fact that $U = \cos \nu$ and $dU = -\sin \nu$)

$$v = \frac{\pi}{3} [r_1^3(2 - 3 \cos \psi + \cos^3 \psi) + r_2^3(2 - 3 \cos \varphi + \cos^3 \varphi)] \quad (\text{S22})$$

while the surface area of the nuclei are the addition of the two following areas

$$a(r_1) = 2\pi r_1^2(1 - \cos \psi) \quad (\text{S23})$$

$$a(r_2) = 2\pi r_2^2(1 - \cos \varphi) \quad (\text{S24})$$

$$a(R) = 2\pi R^2(1 - \cos \chi) \quad (\text{S25})$$

We can derive the following geometrical relationships (see Fig. S.5),

$$R^2 = x^2 + \overline{OO_x}^2 \quad (\text{S26})$$

$$r_1^2 = x^2 + \overline{O_1O_x}^2 \quad (\text{S27})$$

$$r_2^2 = x^2 + \overline{O_2O_x}^2 \quad (\text{S28})$$

$$\cos \chi = \frac{\overline{OO_x}}{R} \quad (\text{S29})$$

$$\cos(\pi - \psi) = \frac{\overline{O_1O_x}}{r_1} \quad (\text{S30})$$

$$\cos \varphi = \frac{\overline{O_2O_x}}{r_2} \quad (\text{S31})$$

From these equations we can write

$$R^2(1 - \cos^2 \chi) = r_1^2(1 + \cos^2 \psi) = r_2^2(1 - \cos^2 \varphi) \quad (\text{S32})$$

Consequently

$$\cos \chi = \sqrt{1 - \left(\frac{r_2}{R}\right)^2 (1 - \cos^2 \varphi)} \quad (\text{S33})$$

$$\cos \psi = \sqrt{\left(\frac{r_2}{r_1}\right)^2 (1 - \cos^2 \varphi) - 1} \quad (\text{S34})$$

If $d = \overline{O_1O_2}$, then

$$d^2 = l_1^2 + (r_2 - \delta_2)^2 \quad (\text{S35})$$

$$r_1^2 = \delta_2^2 + l_1^2 = r_1^2 \cos^2(\pi - \theta) + l_1^2 = r_1^2 \cos^2(\theta) + l_1^2 \quad (\text{S36})$$

The two equations lead to (following the approach of Qian and Ma⁷)

$$d = \sqrt{r_1^2 + r_2^2 + 2r_1r_2 \cos \theta} \quad (\text{S37})$$

We can calculate that

$$\cos \psi = \frac{r_2 \cos \theta + r_1}{d} \quad (\text{S38})$$

$$\cos \varphi = \frac{r_2 + r_1 \cos \theta}{d} \quad (\text{S39})$$

At the critical radii r_1^* and r_2^* the system is at equilibrium and we have $P_g^* = P_v$ as well as the Laplace equations verified at all interfaces:

$$P_v = P_l^* + \frac{2\gamma_{gl}(r_1^*)}{r_1^*} \quad (\text{S40})$$

$$P_v = P_A^* + \frac{2\gamma_{gc}(r_2^*)}{r_2^*} \quad (\text{S41})$$

$$P_l^* = P_A^* + \frac{2\gamma_{lc}}{R} \quad (\text{S42})$$

For nucleation occurring on the surface of an encapsulated water droplet, we have

$$P_l^* = P_A^* - \frac{2\gamma_{lw}}{R} \quad (\text{S43})$$

The Eq. S41 and S42 gives

$$r_2^* = \frac{2\gamma_{gc}(r_2^*)}{(P_v - P_l^*) + \frac{2\gamma_{lw}}{R}} \quad (\text{S44})$$

while Eq. S40 gives

$$r_1^* = \frac{2\gamma_{gl}(r_1^*)}{(P_v - P_l^*)} \quad (\text{S45})$$

In addition, both radius are linked by the equation (using Eq. S44 and S45))

$$r_2^* = \frac{\gamma_{gc}(r_2^*)}{\frac{\gamma_{gl}(r_1^*)}{r_1^*} + \frac{\gamma_{lc}}{R}} \quad (\text{S46})$$

In addition,

$$\gamma_{gl}(r_1^*) = \frac{\gamma_{gl}}{1 + \frac{2\delta}{r_1^*}} \quad (\text{S47})$$

$$\gamma_{gc}(r_2^*) = \frac{\gamma_{gc}}{1 + \frac{2\delta}{r_2^*}} \quad (\text{S48})$$

where δ is the Tolman length. Consequently, Eq. S44 and S40 become

$$r_1^* = \frac{2\gamma_{gl}}{(P_v - P_l^*)} - 2\delta \quad (\text{S49})$$

$$r_2^* = \frac{2\gamma_{gc}}{(P_v - P_l^*) + \frac{2\gamma_{lc}}{R}} - 2\delta \quad (\text{S50})$$

Finally, the interfacial tensions should verify the equation (for both a concave or a convex surface)

$$\gamma_{gl}(r_1^*) \cos \psi^* - \gamma_{lc} \cos \chi^* + \gamma_{gc}(r_2^*) \cos \varphi^* = 0 \quad (\text{S51})$$

We calculate $\cos \theta^*$, by inserting the values of $\cos \chi^*$ (Eq. S33), $\cos \psi^*$ (Eq. S38) and $\cos \varphi^*$ (Eq. S39) in Eq. S51

$$\begin{aligned} & \left(\gamma_{gl}^2(r_1^*)r_2^{*2} + 2\gamma_{gl}\gamma_{gc}(r_2^*)r_1^*r_2^* + \gamma_{gc}^2(r_2^*)r_1^{*2} - \frac{\gamma_{lc}^2 r_1^{*2} r_2^{*2}}{R^2} \right) \cos^2 \theta^* \\ & + (2\gamma_{gl}^2(r_1^*)r_1^*r_2^* + 2\gamma_{gl}(r_1^*)\gamma_{gc}(r_2^*)r_1^{*2} + 2\gamma_{gl}(r_1^*)\gamma_{gc}(r_2^*)r_2^{*2} + 2\gamma_{gc}^2(r_2^*)r_1^*r_2^* - 2\gamma_{lc}^2 r_1^* r_2^*) \cos \theta^* \\ & + \gamma_{gl}^2(r_1^*)r_1^{*2} + 2\gamma_{gl}(r_1^*)\gamma_{gc}(r_2^*)r_1^*r_2^* + \gamma_{gc}^2(r_2^*)r_2^{*2} - \gamma_{lc}^2 r_1^{*2} - \gamma_{lc}^2 r_2^{*2} + \frac{\gamma_{lc}^2 r_1^{*2} r_2^{*2}}{R^2} = 0 \end{aligned} \quad (\text{S52})$$

It is a second order equation $a \cos^2 \theta^* + b \cos \theta^* + c = 0$ where the solutions are

$$\cos \theta^* = \frac{-b \pm \sqrt{b^2 - 4ac}}{2a} \quad (\text{S53})$$

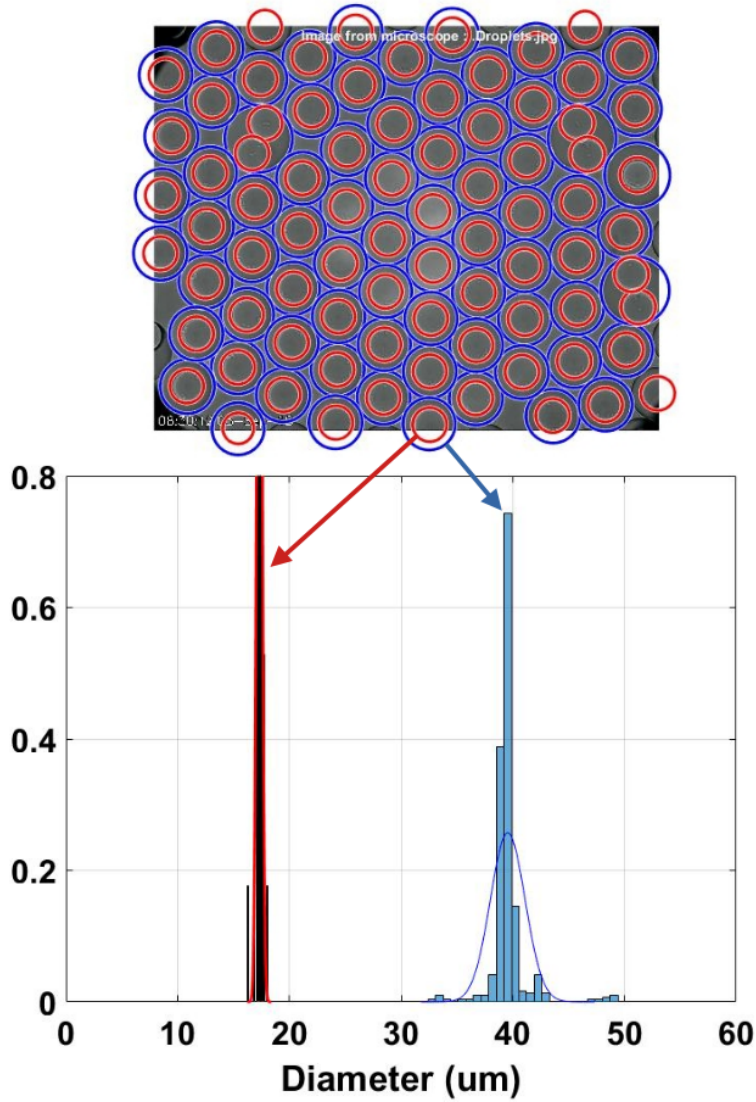


Figure S.1: Characterization of core shell droplets with the water volume fraction of $\varphi_w \approx 0.1$. The red circles delimit the water core and the blue circles the outer surface of the droplets. The measurements carried out on 75 droplets and fitted by a Gaussian distribution led to the following results: the external droplet radius $R = 20.3 \mu\text{m}$ and the polydispersity, $\text{PDI} = (\sigma/\mu)^2 \approx 3 \times 10^{-3}$, where σ and μ are respectively the standard deviation and the mean value. The internal water radius $R_w = 9.1 \mu\text{m}$ and $\text{PDI} \approx 6 \times 10^{-4}$.

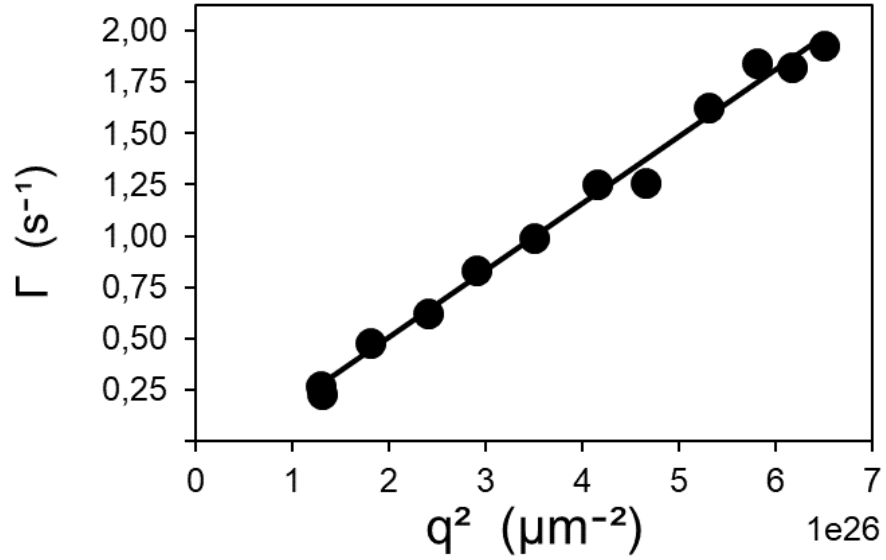


Figure S.2: The data represent Dynamic Light Scattering measurements performed on an emulsion prepared by high-pressure microfluidizer. The linear fit of Γ_θ versus q^2 leads to $R = 74.5 \pm 2$ nm and to a polydispersity index $\text{PDI} = 0.12 \pm 0.06$, knowing that a sample is considered monodisperse when $\text{PDI} < 0.2$.

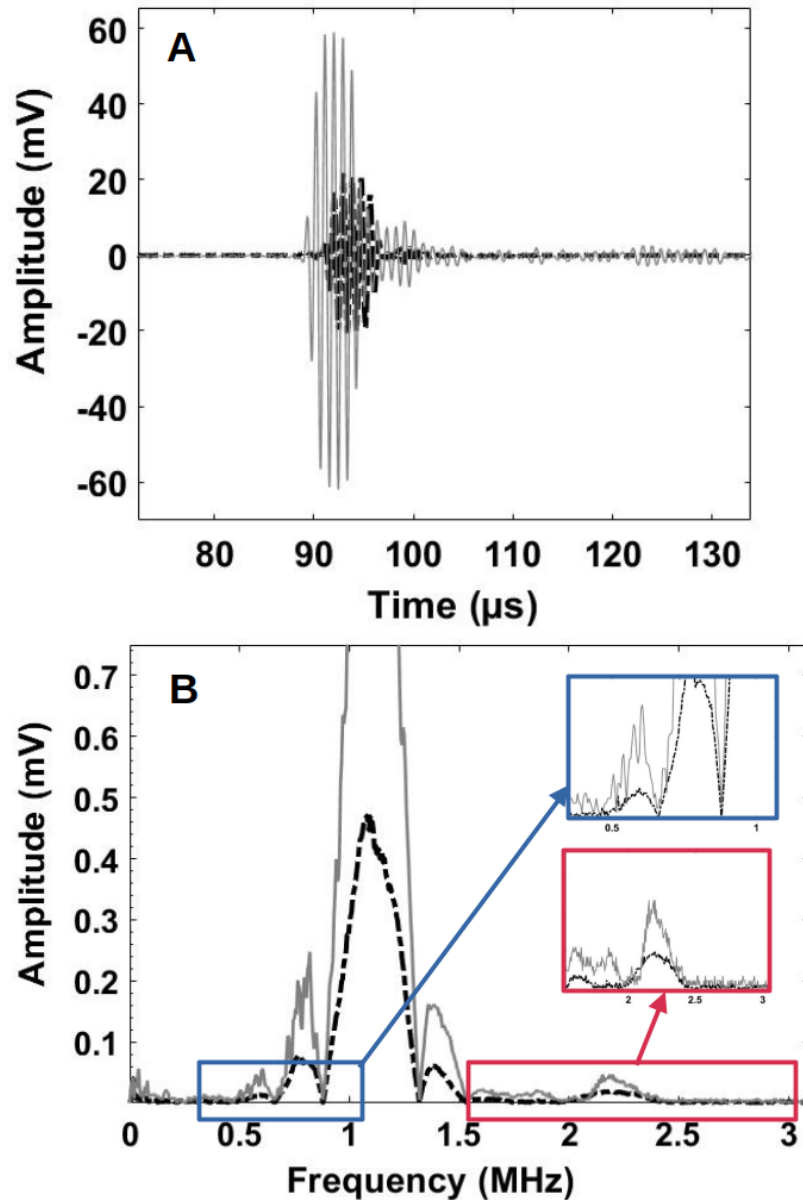


Figure S.3: In these experiments, plain PFH droplets of radius $R = 20 \mu\text{m}$ were used in glycerol at 20°C with $P = 2 \text{ MPa}$ and $f_0 = 1.1 \text{ MHz}$. (A) Signals emitted by a sample, containing either glycerol (black) or PFH bubbles in glycerol (grey). (B) Fourier transforms of the mean values of 300 signals represented in (A). Insets: magnifications of the signals in the vicinity of 0.55 and 2.2 MHz, respectively.

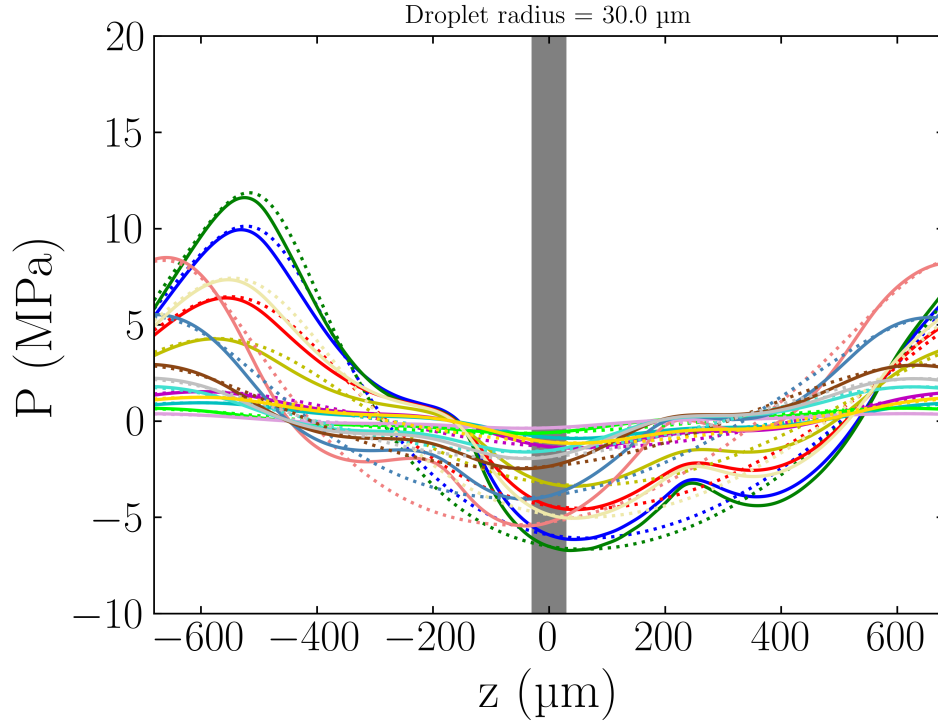


Figure S.4: Variation of the pressure wave in the presence of a droplet (solid lines) and in the absence of a droplet (dotted lines) along the z axis (i.e. $\theta = 0$ or π , and $0 < r < R$). The different color lines correspond to various intensities given to the transducer in the HIFU-beam simulator script. The grey band indicates the radius of the droplet, that is $30 \mu\text{m}$ in this figure. The calculation was performed for z spanning over the acoustic wavelength (i.e. c/f). The lines are snapshots of the wave where t varies over a wave period $T = 1/f$ and for which the pressure inside the droplet is the minimal.

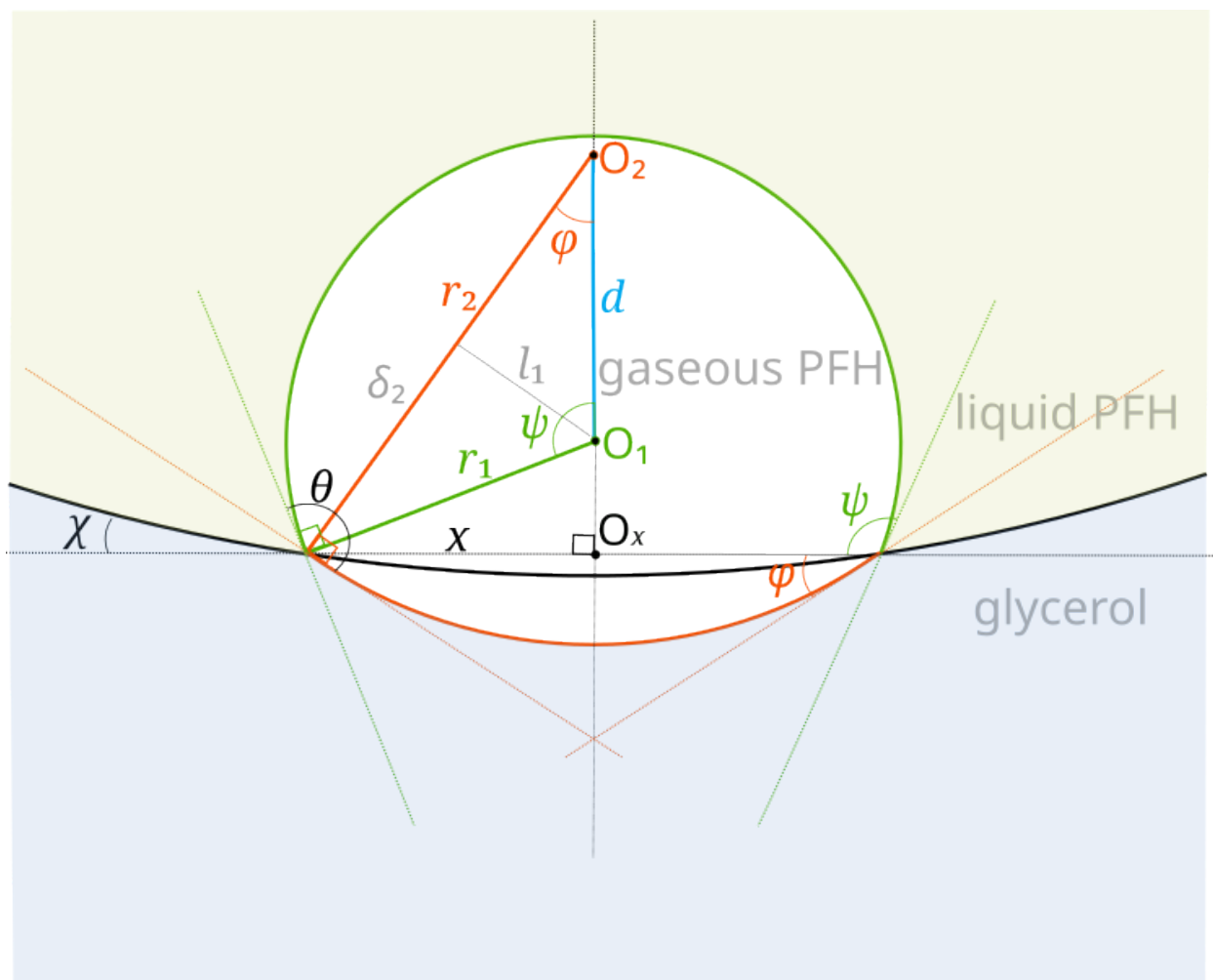


Figure S.5: schema of a nucleus on the plain PFH droplet surface, in contact with water.

References

- (1) Castillo, E.; Hadi, A.; Balakrishnan, N.; Sarabia, J. *Extreme Value and Related Models With Applications in Engineering and Science*; Wiley, 2005.
- (2) David, H. A.; Nagaraja, H. N. *Order Statistics*; Wiley Series in Probability and Statistics; Wiley, 2004.
- (3) Embrechts, P.; Klüppelberg, C.; Mikosch, T. *Modelling Extremal Events for Insurance and Finance*; Springer-Verlag, 1997.
- (4) Toshev, S.; Milchev, A.; Stoyanov, S. On some probabilistic aspects of the nucleation process. *J. Cryst. Growth* **1972**, *13-14*, 123–127, Third International Conference on Crystal Growth.
- (5) Skripov, V.; Kondor, R.; Slutzkin, D. *Metastable Liquids*; A Hasted Press book; J. Wiley, 1974.
- (6) Blander, M.; Katz, J. L. Bubble nucleation in liquids. *AIChE J.* **1975**, *21*, 833–848.
- (7) Qian, M.; Ma, J. The characteristics of heterogeneous nucleation on concave surfaces and implications for directed nucleation or surface activity by surface nanopatterning. *J. Cryst. Growth* **2012**, *355*, 73–77.